THIRD INTERIM TECHNICAL REPORT

For The

STUDY ON INTEGRATION OF SILVER-ZINC BATTERY IMPROVEMENTS

(1 March 1969 — 31 December 1969)

Contract No.: NAS 5-11579

Prepared By
HUGHES AIRCRAFT COMPANY
AEROSPACE GROUP
Space Systems Division
Propulsion And Power Systems Laboratory
El Segundo, California

For
GODDARD SPACE FLIGHT CENTER
Greenbelt, Maryland

Hughes Ref. No. 70(22)-3276/B6700 ▪ SSD 00181R

THIRD INTERIM TECHNICAL REPORT

For The

STUDY ON INTEGRATION OF SILVER-ZINC BATTERY IMPROVEMENTS

(1 March 1969 — 31 December 1969)

Contract No.: NAS 5-11579

GODDARD SPACE FLIGHT CENTER
Contracting Officer: A. L. Essex
Technical Monitor: W. H. Webster

Prepared By
HUGHES AIRCRAFT COMPANY
AEROSPACE GROUP
Space Systems Division
Propulsion And Power Systems Laboratory
El Segundo, California

For
GODDARD SPACE FLIGHT CENTER
Greenbelt, Maryland

Project Manager: P.S. DuPont
For
GODDARD SPACE FLIGHT CENTER
Greenbelt, Maryland

Prepared By: R J Haas
R. J. Haas
Unit Engineer

R.A. Steinhauer
R.A. Steinhauer
Project Engineer

Approved By: P. S. duPont
P.S. DuPont
Project Manager

Hughes Ref. No. 70(22)-3276/B6700 ▪ SSD 00181R

ABSTRACT

This report covers the technical progress and status on Goddard Space Flight Center contract NAS 5-11579 for the period of 1 March 1969 through 31 December 1969. During this period batteries were fabricated and tested. Many of the separately developed silver-zinc improvements when incorporated into one battery have been both beneficial and detrimental. A complete status is reported herein.

CONTENTS

ILLUSTRATIONS

TABLES

1.0 INTRODUCTION

This report covers the 10-month period of activity from 1 March 1969 through 31 December 1969. Originally this contract was scheduled for completion in December 1969, but an increase to the scope of work now extends this contract through December 1970. This increased work scope permits further study and fabrication of six additional batteries that will incorporate the cell core construction developed, during Phases I and II of this contract, in five-cell batteries using single cell cases rather than in the monoblock battery cases currently used. Because of this contractual change in schedule and work scope, this report, originally scheduled to be a Final Technical Report, is issued as the Third Interim Technical Report for this program.

During this reporting period, a total of seven batteries plus one engineering prototype battery were fabricated. The contract hardware delivery requirement through December 1969 is for six batteries. Battery failures required the construction of an additional battery. The failure mechanism has been established and is reported herein.

All batteries after formation cycling in a vented condition were then hermetically sealed prior to performance and characterization testing at ambient temperatures of 77° and 32° F. A total of three batteries successfully completed final capacity tests and were shipped to the Goddard Space Flight Center, completing Phase II of this program. In lieu of delivery of three of the six batteries, it was agreed that a failure analysis would be performed on the batteries not meeting minimum acceptance criteria.

2.0 TECHNICAL DISCUSSION

2.1 FABRICATION TECHNIQUES

2.1.1 Cell Core

Two different separator configurations were incorporated into the six, five-cell, monoblock batteries. The first included five layers of Radiation Associates Incorporated Permion 2291 polyethylene separator and one layer of 0.001 inch thick Webril Dynel EM 470 absorber next to the positive plates. The second configuration was the same except that it incorporated a 0.0013 inch thick electrodeposited coating* of calcium hydroxide on the surface of the silver plates to reduce the rate of silver migration through the separator system and only four layers of 2291 separator to allow for the added thickness of the calcium hydroxide.

The cell core fabrication process starts with the selected number of layers of separator plus absorber material being placed between two metal plates that are slightly larger than the outer dimensions of the separator frames. These materials are then cut with a hot knife to the size of the metal plates, producing thermally bonded separator-absorber blanks. The bond is along the periphery of the blanks and although not a complete heat seal it quite adequately retains the four or five layers of 2291 separator and one layer of absorber together throughout subsequent fabrication procedures. One of the separator-absorber blanks produced by this process is shown in Figure 1.

The separator-absorber blanks, separator frames (Figure 2), and positive and negative plates all are stacked together as shown in Figure 3. Once the cell cores are stacked and clamped (see Figure 4), the extended edges of the blanks are trimmed to the surface produced by the aligned stack of separator frames. The resultant cell core then is conformally coated with epoxy, thereby completing fabrication of the cell core subassembly (see Figure 5).

---

*Process developed at General Electric Research Laboratories by W.N. Carson, Jr., et al.

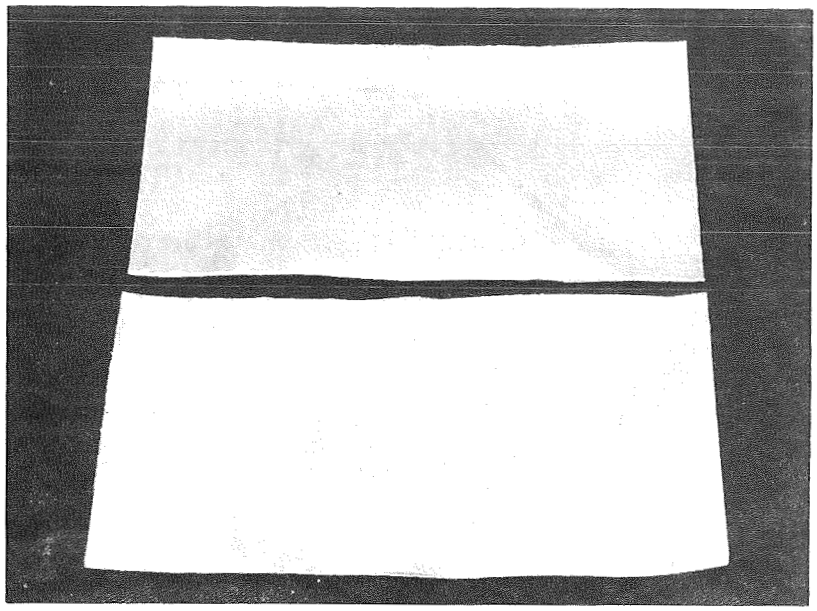

Figure 1. Hot Knife Cut Multilayer Separator Blanks
(Photo A24866)

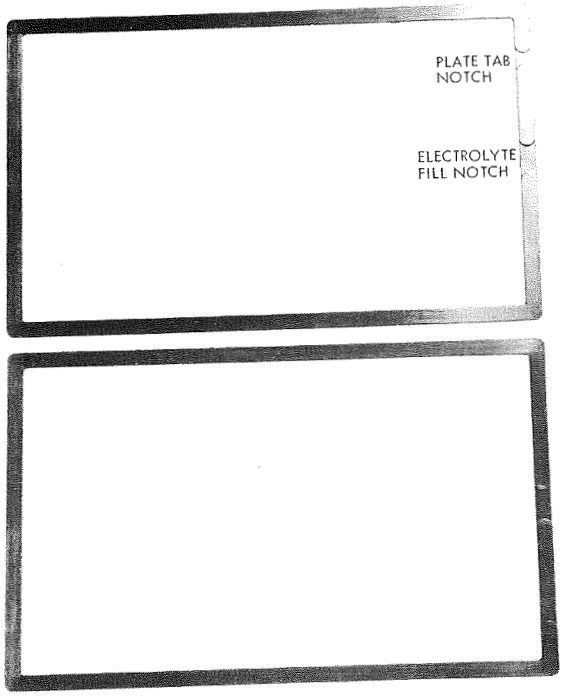

Figure 2. Injection Molded Separator Frames
(Photo A24845)

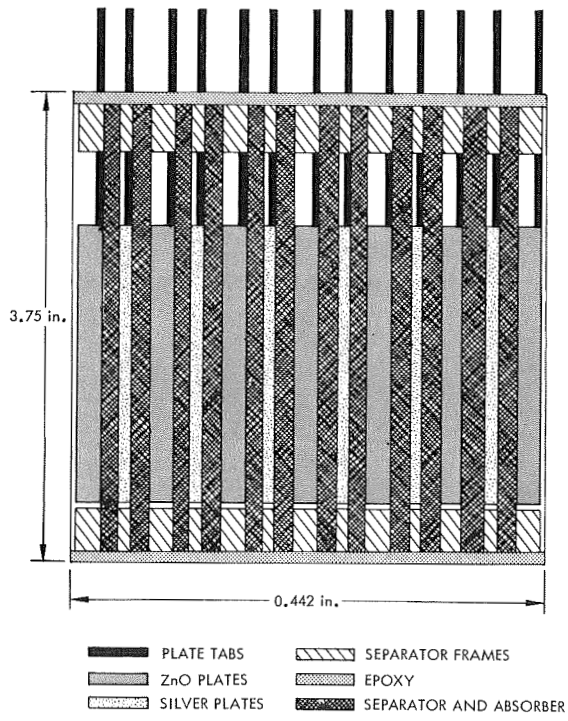

Figure 3. Cross Section of Cell Core Assembly

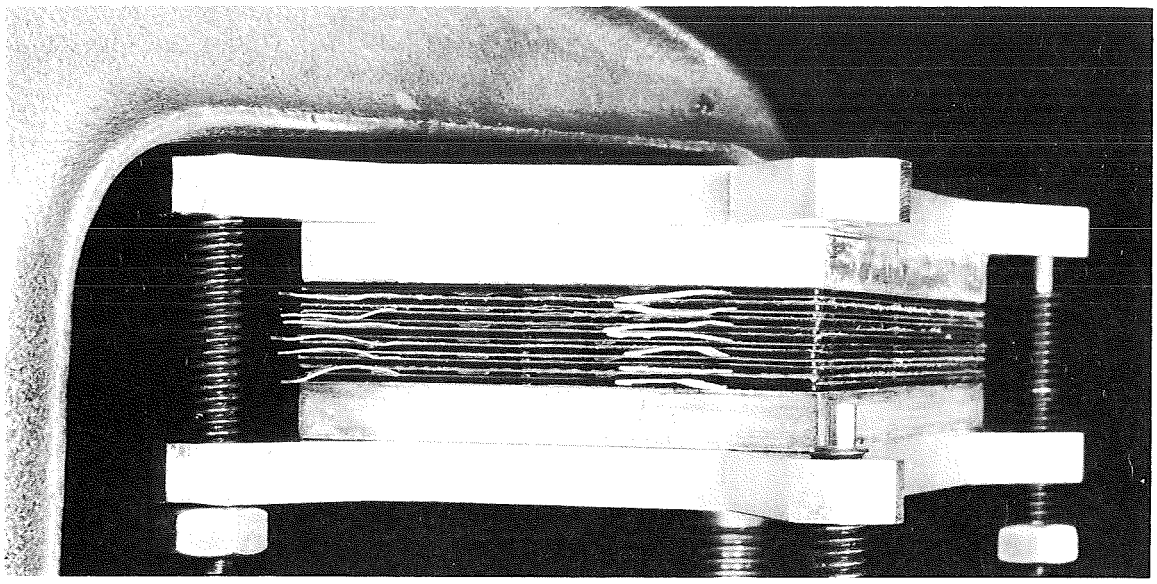

Figure 4. Cell Core Clamped in Tooling Prior to Application of Epoxy

(Photo A24872)

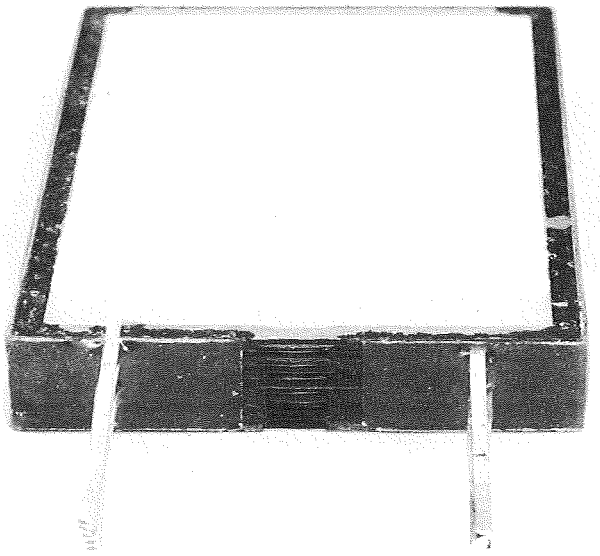

Figure 5. Completed Cell Core

(Photo A24846)

It is considered that the following conditions have contributed to cell and battery failures reported herein.

1) A one-quarter of an inch foldback of the expanded metal grid at the periphery of the negative plates was used to inhibit edge crumbling.

2) The cell core is clamped prior to and during the trimming and application and curing of the conformal epoxy coating.

2.1.2 Battery Case

The five-cavity monoblock battery case was successfully injection molded by Jupiter Engineering, Menlo Park, California after solving the following problems:

1) Core shifting that affected wall thicknesses

2) Air entrapment causing voids in the battery case, primarily in the outermost walls

3) Part ejection from the mold

It was necessary to change the gate geometry, install two, 0.25 inch diameter pilot pins into each of the five mold cores, and to include fill channels for the thermoplastic on the outer surface of the end walls of the monoblock case in order to produce an acceptable part. The pilot pins mate with the opposing mold base and prevent any lateral shifting of the five cores. Smaller diameter pins simply sheared under the injection molding pressures. Gate geometry, the number of gates, their relative diameters, and locations had to be optimized to prevent unfavorable interactions that resulted in voids in the case walls. Wall numbers 2 and 5 originally caused the greatest problems with regard to core shifting; however, wall numbers 1 and 6 contained void areas that could not be eliminated until fill channels were incorporated in the tooling. Refer to Figure 6, for wall reference numbers.

This case design was developed to:

1) Save battery packaging weight by use of a five-cell monoblock with thin walls

2) Incorporate minimum draft angle walls for enhancement of battery performance through improved plate-separator-electrolyte interfaces.

The monoblock case is much more difficult to eject from its mold than is a single cavity case because there is five times the surface area upon which the case can seize onto its mold. Further, the thin walls, i.e., 0.080 to 0.110 inch thick, and the minimum interior draft angle increase

the difficulty of case removal from the mold. The mold cores required a high quality surface polish and the use of mold release to facilitate part removal from the tooling at the conclusion of the injection molding cycle.

The monoblock case drawing required the interior draft angle to be within 0.1 to 0.2 degree per wall, maximum. The interior cavities are held to a change in dimension from top to bottom in the widthwise direction of no more than 0.023 inch over the 4.500 inches height of the case. Again, this was done to enhance the internal interfaces of the cell cores to produce optimum performance characteristics, but it contributed to the difficulties encountered in the injection molding process.

The pilot pins required to prevent core shifting produced two holes in each cell cavity. These holes were filled with injection molded press fit plugs that were epoxy bonded into place. No electrolyte leakage has been observed at the location of these epoxy bonded plugs (see Figure 7).

2.1.3 Intercell and Intracell Connectors

All intracell and intercell electrical connections were accomplished by use of the machined copper parts x3182884 and x3182885. Copies of these drawings were included in the appendix of the Second Interim Report of this contract. All of the silver tabs from both the positive and negative plates of each of the five cells were fed through their respective slots in the machined Noryl thermoplastic cover. The copper connecting parts were put into place and silver soldered, effecting individual plate tab connections for each cell, the intercell connections required to form a battery, and all necessary instrumentation wiring. These copper connectors and all individual plate tabs were epoxied into the channel designed for that purpose, thereby producing the first seal at the location of the cover plate tabs.

All of the instrumentation wiring and lead wires then were positioned prior to the filling of both channels with epoxy that encapsulated these wires and provided a second seal. Figure 8 shows how these processes occurred.

2.1.4 Common Gas Manifold and Gas Recombination Assembly

A common gas manifold was machined into the battery cover. This was done for two reasons:

1) The Surveyor main battery probably was the first silver-zinc secondary battery to use a common gas manifold. This was done to equilibrate pressures between all cells of the battery and to permit the use of a single pressure transducer. The pressure transducer's voltage signal was used in an override control circuit to facilitate charge termination in case anomalous battery performance caused the internal gas pressure to build up to untolerable levels. While this override was not required to operate during any of the Surveyor missions, it still was considered by Hughes Aircraft Company to be a valuable reliability and safety feature.

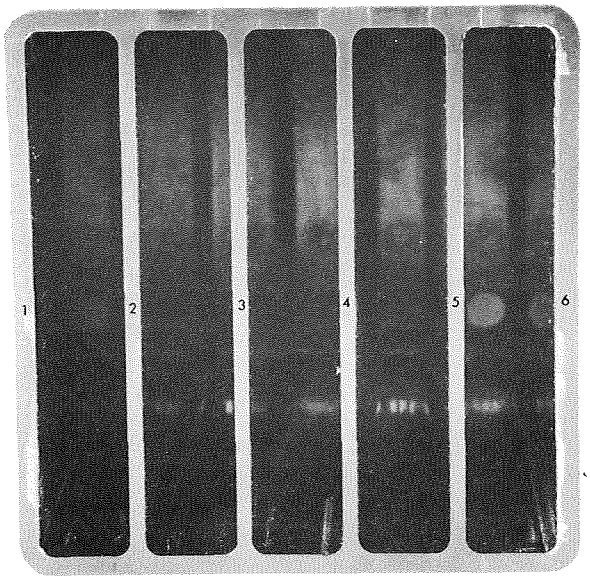

Figure 6. Top View of Injection Molded Case

(Photo A24856)

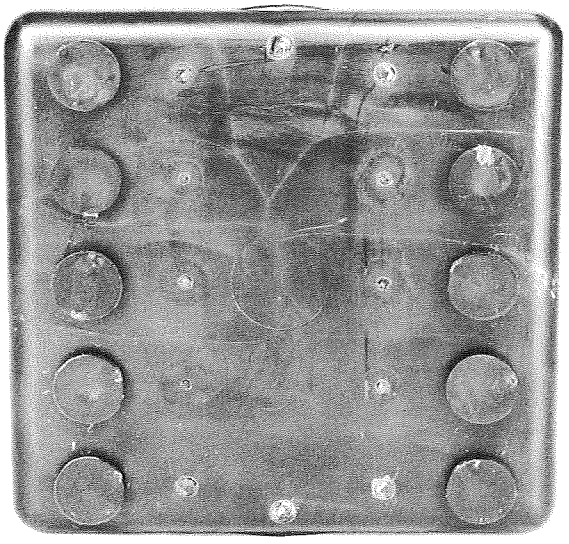

Figure 7. Case Bottom Showing Gates, Pilot Pin Plugs, and Thermoplastic Fill Channel on Outer Walls

(Photo A24844)

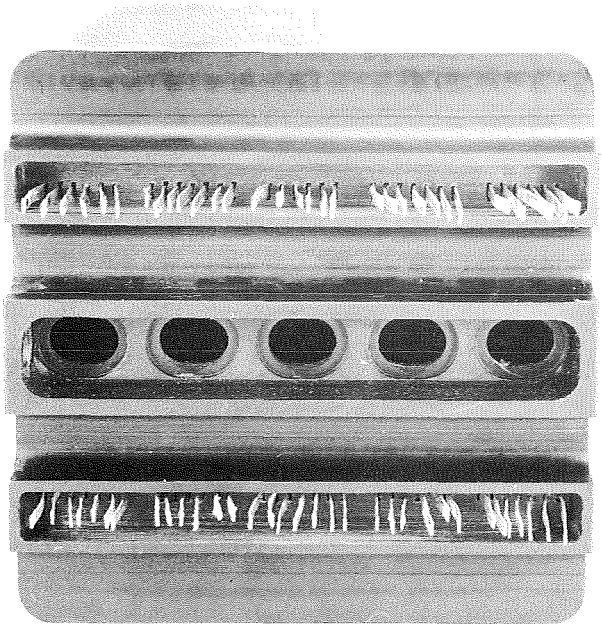

a) Plate Tabs Inserted Through Cover
(Photo A24852)

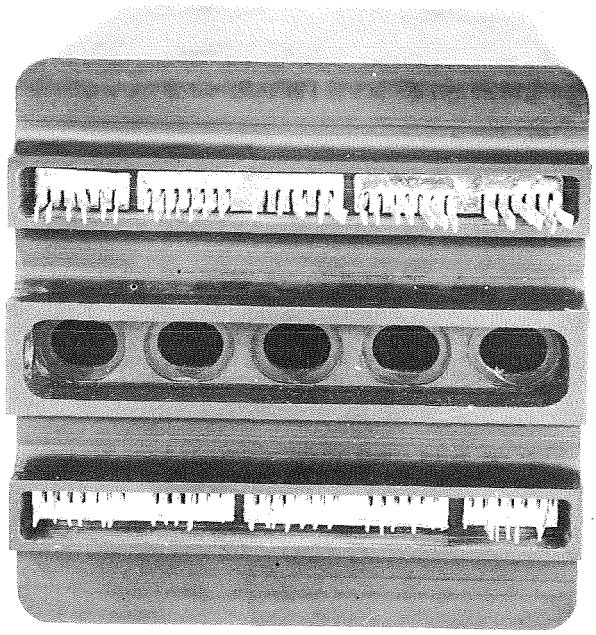

b) Copper Intercell and Intracell Connectors in Place
(Photo A24855)

c) Instrumentation and Lead Wires Connected
(Photo A24850)

Figure 8. Battery Case Cover

2) The common gas manifold used on the batteries for this program was required to permit the use of the gas recombination assembly, described below, on a battery basis rather than on an individual cell basis.

The use of a common gas manifold in a secondary silver-zinc battery requires that precautions be taken to avoid the possibility of a common electrolyte path among the cells of the battery. The Surveyor battery used cellulosic sponges in the orifice between each cell and the common gas manifold. Further, a tortuous gas path was used within the manifold to inhibit electrolyte bridging between cells. The batteries built for this current program, NAS5-11579, did not require a tortuous path manifold because a hydrophobic microporous membrane was epoxied into each orifice between the silver-zinc cells and the common gas manifold. This hydrophobic microporous membrane, Chemplast Incorporated, Zitex E-610-122 (a teflon material) proved successful in retaining electrolyte within each cell while simultaneously permitting any oxygen or hydrogen gases that were generated during battery operation to readily pass through to the common manifold.

Because the partial pressure of water vapor was essentially the same on both sides of the microporous membranes, there was no net water loss from any of the five cells within a battery by this means. The use of this type of membrane within electrochemical cells or batteries for the purpose of restricting electrolyte, but not gases, should be given strong consideration in future applications where segregation of gases and electrolyte may be useful. Further, it is an excellent way to prevent common electrolyte problems that are troublesome in some battery and fuel cell designs.

The gas recombination assembly incorporated the following components:

1) A microfuel cell developed by McDonnell-Douglas' Astropower Laboratory designed for use on a silver-zinc cell to electrochemically getter oxygen or hydrogen gas.

2) A 2.5 amp-hr secondary silver-zinc cell, incorporating Permion 2290 separator, to facilitate charging of the microfuel cell.

3) Rigid plastic tubing for the plumbing required between the microfuel cell, auxiliary 2.5 amp-hr silver-zinc cell, and the battery's gas manifold.

All components of the gas recombination assembly and its subsequent attachment to the battery's gas manifold were adhesively bonded using Epiphen ER 825A epoxy resin. Pressure testing with nitrogen gas for a 24-hour period was the method used to determine whether or not any gas leak paths were present.

The microfuel cell was not designed to operate on a battery basis, but on the basis that one microfuel cell would be used for each silver-zinc cell within a battery. In this program, Hughes has attempted to use one microfuel cell for all five cells of the battery. Therefore, it was necessary to develop a method for recharging the microfuel cell without unbalancing any of the five battery cells. The microfuel cell operates with a small drain rate resistor across the oxygen recombination couple and another resistor across the hydrogen couple. Microfuel cell discharge occurs when oxygen or hydrogen gas generated by the silver-zinc battery is recombined by the microfuel cell. Microfuel cell charging can be accomplished either parasitically or by use of an external power supply. In either case, the microfuel cell must be electrically connected both externally by physical means and internally through a common electrolyte path to a silver-zinc cell. If the microfuel cell is connected and charged through one of the cells of the battery, that cell will become unbalanced with respect to capacity in comparison with the other cells in the same battery. To circumvent this problem, Hughes has added a 2.5 amp-hr auxiliary cell specifically for the purpose of microfuel cell charging. This auxiliary cell prevents the imbalance of any of the five cells of the battery when the microfuel cell is charged, but there still is some concern that gases recombined during battery operation might be regenerated during the next charge operation required for the microfuel cell. Because the battery and the gas recombination assembly are a closed system, this could pose a possible insoluble problem.

During battery tests conducted to date utilizing the charge control system described in subsection 2.4.2 of the First Interim Technical Report for this contract, there has not been a sufficient volume of gas generated to require the recharge of the microfuel cell on any of the five cell batteries. Therefore, this problem is speculative at this time as it has not been proven by experimental data acquired to date on the battery assemblies for this program.

Photographs of the battery cover and its common gas manifold, the gas recombination assembly, and a three-quarter view of the engineering model battery assembly are included as Figures 9, 10, and 11.

2.1.5 Connector

The nonmagnetic connectors supplied to Hughes Aircraft Company by the Goddard Space Flight Center as Government-furnished equipment were mounted on specially machined Noryl thermoplastic brackets. These brackets were previously adhesively bonded with epoxy to the battery case as shown in Figures 12 and 13. It should be noted that the deliverable batteries incorporated Noryl thermoplastic injection molded cases that are opaque. The photographs that show a transparent battery case are those of the engineering prototype battery that used a styrene acrylonitrile case. The transparent SAN case permitted observation of the mechanical structures as they would be situated in the final battery cases. This was planned in case a mechanical interference problem occurred that could not otherwise be observed and solved.

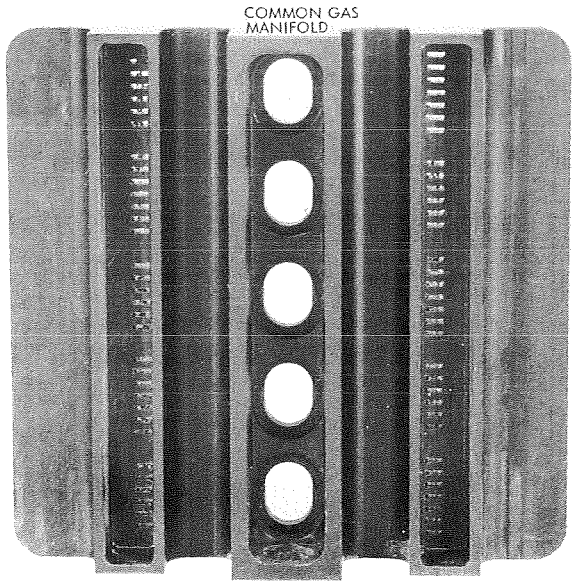

Figure 9. Battery Cover with Common Gas Manifold

(Photo A24854)

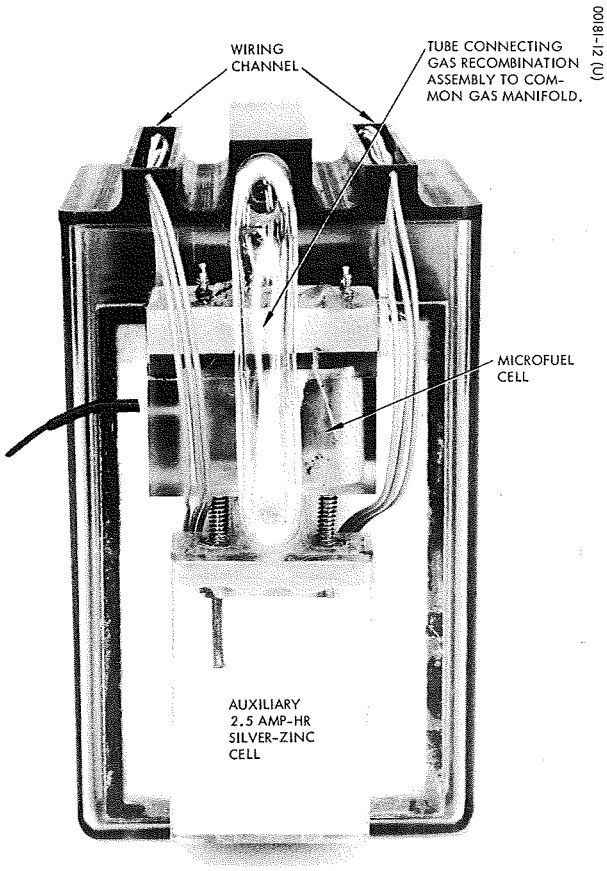

Figure 10. Gas Recombination Assembly

(Photo A24847)

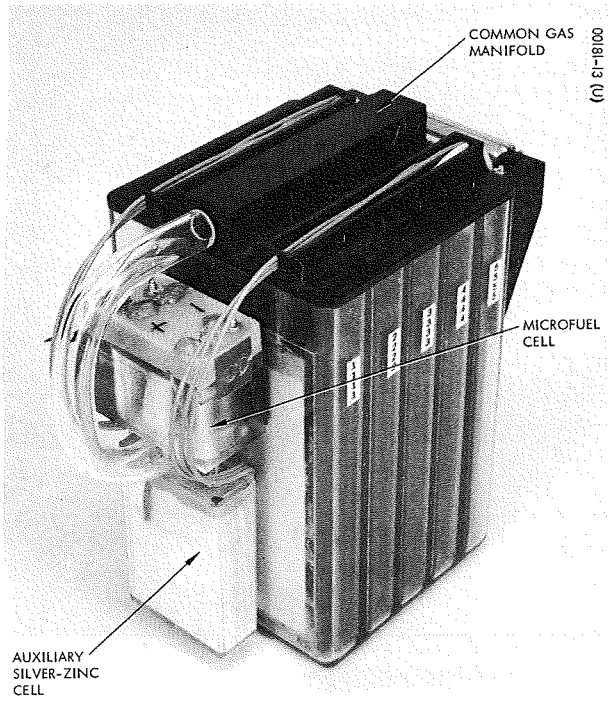

Figure 11. Three-Quarter View of Engineering Model Battery Assembly

(Photo A24848)

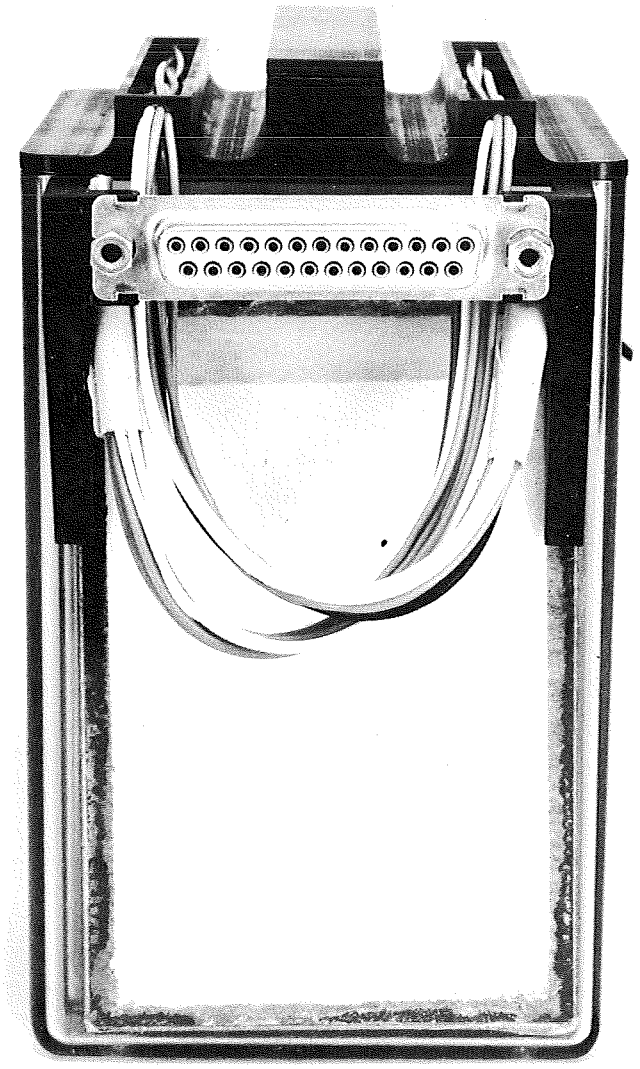

Figure 12. Battery Terminal Connector
(Photo A24849)

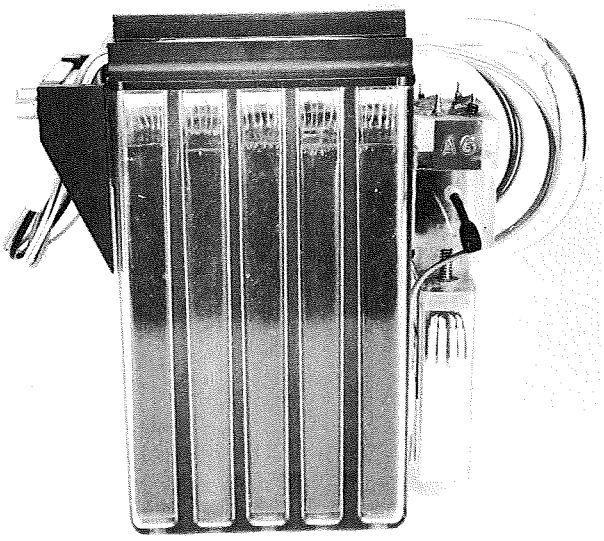

Figure 13. Side View of Complete Battery
(Photo A24851)

The connector pin utilization diagram has been more specifically defined in Figure 14. The pin utilization shown in the Second Interim Technical Report still is applicable, but this is a further refinement of the previous plan.

2.1.6 Battery Fabrication Status

A total of six, five-cell batteries are deliverable on this program through December 1969. Three of these batteries incorporate five layers of Permion 2291 separator, one layer of Webril Dynel EM 470 absorber next to the positive plates, and no calcium hydroxide coating on the silver electrodes. The remaining three batteries contain four layers of Permion 2291 separator, one layer of Webril Dynel EM 470 absorber next to the positive plates, and a 0.0013inch thick electrodeposited coating of calcium hydroxide. Batteries with serial numbers 1 through 3 do not contain calcium hydroxide coated silver plates; batteries with serial numbers 4 through 6 do contain the calcium hydroxide coatings. Because of a performance anomaly that occurred during early formation cycling, battery serial number 2 would not pass the minimum capacity requirement of 12 amp-hr. A new battery was built as a replacement and was assigned serial number 2A. The anomalous performance of battery No. 2 is commented upon further in subsection 2.3.

2.2 ACTIVATION AND PERFORMANCE TEST RESULTS

2.2.1 Activation and Formation

Six batteries were activated by placing 30 milliliters of electrolyte solution in each cell using a vacuum fill technique. The electrolyte solution was saturated with zinc oxide and was a 40 weight percent solution of potassium hydroxide. The batteries were allowed to stand after vacuum filling for 48 hours to assure complete wet out of the separator system and the plates prior to the first formation cycling.

Formation cycling consisted of charging at 1.00 ampere to 2.00 volts per cell, followed by 5.0 amperes discharge to 1.00 volt per cell. A total of three of these formation cycles was required. Three of the six batteries, serial numbers 2, 4 and 6, exhibited anomalous voltage behavior during the charge portion of the formation cycling and were eliminated from further testing. These batteries were failure analyzed and the results are reported later in subsection 2.3.

A replacement battery, serial number (S/N) 2A, was fabricated and substituted for battery S/N 2. Replacements for the other two batteries, S/N's 4 and 6, could not be fabricated because of lack of battery covers and calcium hydroxide plates in time to meet the program schedule. Autopsy results indicated a problem related to the negative plates that could not be corrected without procuring new redesigned plates; therefore, replacement batteries were not built for S/N's 4 and 6. The data obtained during the three formation cycles completed on batteries 1, 2A, 3 and 5, are shown in Table 2-1.

The measured ampere-hour capacity of batteries 1 and 3 during the third formation cycle was somewhat lower than that of the previous cycles. These batteries received incomplete charge during this cycle because a test equipment malfunction terminated charge at 1.93 volts per cell average rather than 2.00 volts per cell. The capacity subsequently delivered by these batteries during test cycles 4 and 5 compares favorably with that of the other batteries, as evidenced by the data listed in Table 2-2.

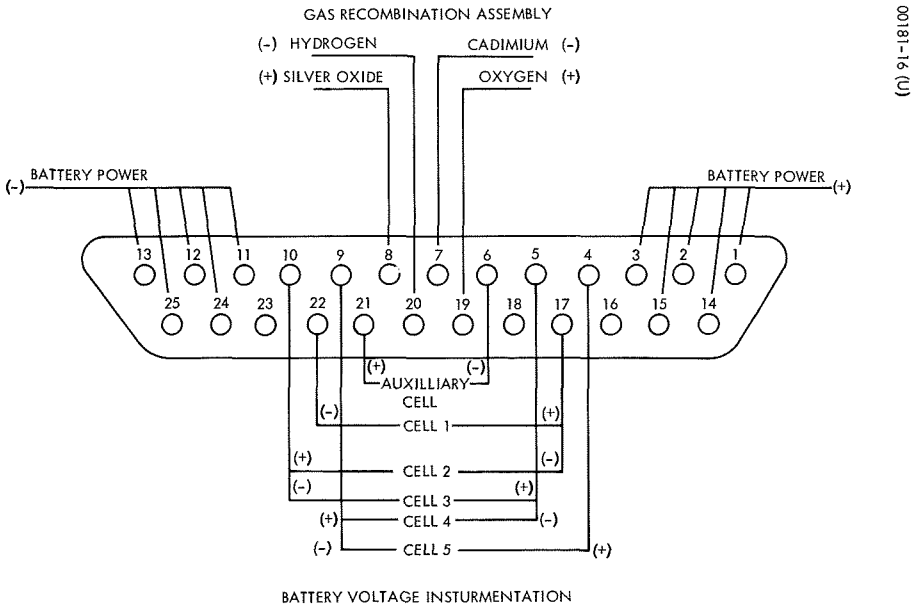

Figure 14. Connector Pin Utilization

TABLE 2-1. BATTERY FORMATION CYCLE DATA

Battery S/N	Capacity, ampere-hours			
	Cycle No. 1	Cycle No. 2	Cycle No. 3	Average
1	18.0	22.0	14.5	18.2
2A	15.8	18.5	17.5	17.9
3	17.0	20.0	14.0	17.0
5	16.0	15.8	19.0	16.9

The gas recombination assemblies were prepared for operation by the addition of electrolyte and use of a low rate charge procedure prior to permanently sealing the battery's gas manifold system into its final closed loop configuration. An electrolyte solution of 40 weight percent potassium hydroxide was used in the gas recombination assembly. A charge rate of 10 milliamperes was used. The capacity of the gas recombination assembly is approximately 2.5 amp-hr. This is equivalent to 523 milliliters of oxygen and 1046 milliliters of hydrogen at standard temperature and pressure conditions.

2.2.2 Performance Tests

In all performance tests, and previously in the formation cycling, all overvoltage and undervoltage termination points are based upon the first cell in the five-cell battery that reaches the preselected value. All formation and performance test charging was at the 1.00 ampere charge rate to a 1.98 volts per cell upper voltage cutoff. Performance tests through test cycle No. 5, did not include trickle charging at the 1.87 volts per cell clamp level. However, the tests run after that point, in particular, the ten, 24-hour orbit test cycles run at 25° C and the ten similar test cycles run at an ambient temperature of 0° C, included the described trickle charge from the time the first cell reached 1.98 volts until the completion of that 24-hour period just prior to the start of the next discharge.

2.2.2.1 Capacity

Batteries 1, 2A, 3 and 5 delivered more than their rated capacity of 12 amp-hr during initial formation and exercise cycling. The formation cycling discharge consisted of discharging the batteries at a current of 5.0 amperes to a 1.00 volt per cell cutoff. The discharge portion of cycle 4 was run with a discharge current of 5.0 amperes to a 1.30 volts per cell cutoff, cycle 5 was run at a discharge current of 7.2 amperes to 1.00 volt per cell cutoff. The data from the fourth and fifth discharge cycles are listed in Table 2-2.

TABLE 2-2. AMPERE-HOUR CAPACITY AND VOLTAGE PERFORMANCE FOR CYCLES 4 AND 5

Battery Number	Cycle No. 4		Cycle No. 5	
	Capacity, amp-hr	Mid-Point Discharge Voltage	Capacity, amp-hr	Mid-Point Discharge Voltage
1	19.8	7.454	17.8	7.423
2A	17.3	7.379	17.8	7.240
3	17.5	7.441	17.8	7.428
5	17.1	7.411	14.3	7.427
Average of all batteries	18.9	7.444	16.9	7.379

It should be noted that while the delivered ampere-hour capacity for battery No. 5 is somewhat lower than that of batteries 1, 2A and 3, this is not believed to be attributable to the use of the electrodeposited calcium hydroxide coatings on the silver plates of this battery. Subsequent failure analysis of battery No. 5 indicates another problem was developing. This is reported upon in subsection 2.3.

2.2.2.2 24-Hour Orbit

Batteries 1 and 5 were selected for the 24-hour orbit cycle tests. This was done to allow evaluation of the two different separator configurations, i.e., with and without electrodeposited calcium hydroxide coated silver plates. The following operating parameters were monitored and recorded on a 300 channel automatic data acquisition system:

1) Battery voltage

2) Battery current

3) Cell voltages (each of five cells)

4) Battery temperature

5) Oxygen recombination cell current

6) Hydrogen recombination cell current

The charge procedure developed and recommended by the Goddard Space Flight Center was used as described here:

1) Charge at 1.00 ampere until any cell of the five-cell battery reaches the voltage clamp point of 1.98 volts and the battery charge current drops to 160 milliamperes under this voltage clamped condition.

2) Once step No. 1 is completed, change the charge voltage clamp level to 1.87 volts per cell and continue with this resultant trickle charge for the remainder of the 23-hour charge period.

Discharge consisted of 7.2 amperes constant current for 1.0 hour. The reason for this charge procedure is to reduce oxygen generation to a minimum level.

The batteries were run through ten of the above described test cycles at 25°C (77°F). Then each cell of both batteries was discharged by placing a 2.0-ohm resistor across the connector pins leading to the instrumentation wiring for that cell to minimize cell imbalance prior to the start of the ten test cycles at 0°C (32°F). Cycle test data for the 77°F ambient temperature condition are shown in Figures 15 and 16. It will assist the reader with data interpretation if a correlation chart of cycle number versus the test or procedure is included. This information is summarized in Table 2-3. Cycle test data for the 32°F ambient temperature condition tests are shown in Figures 17 and 18.

TABLE 2-3. CYCLE NUMBER VERSUS TEST OR PROCEDURE

Cycle No(s).	Test or Procedure
1-3	Vented condition. Formation cycles. Charge at 1.00 ampere until first cell of a battery reaches 2.00 volts. Discharge at 5.0 amperes to 1.00 volt per cell.
4-5	Exercise cycles in sealed condition. Charge at 1.00 ampere until first cell of a battery reaches 1.98 volts. Discharge: 4th cycle, 5.0 amperes to 1.30 volts per cell 5th cycle, 7.2 amperes to 1.00 volt per cell
6-15	24-hour orbit cycling of batteries 1 and 5. Charge at 1.00 ampere with a voltage clamp of 1.98 volts per cell and change to trickle charge mode when current drops to 160 milliamperes. Trickle charge for remainder of 23-hour charge period, constant voltage mode at 1.87 volts per cell average. Ambient temperature 25°C (77°F).
16-25	Identical to cycles 6-16, except that ambient temperature is 0°C (32°F).
26	Final capacity check at 25°C.

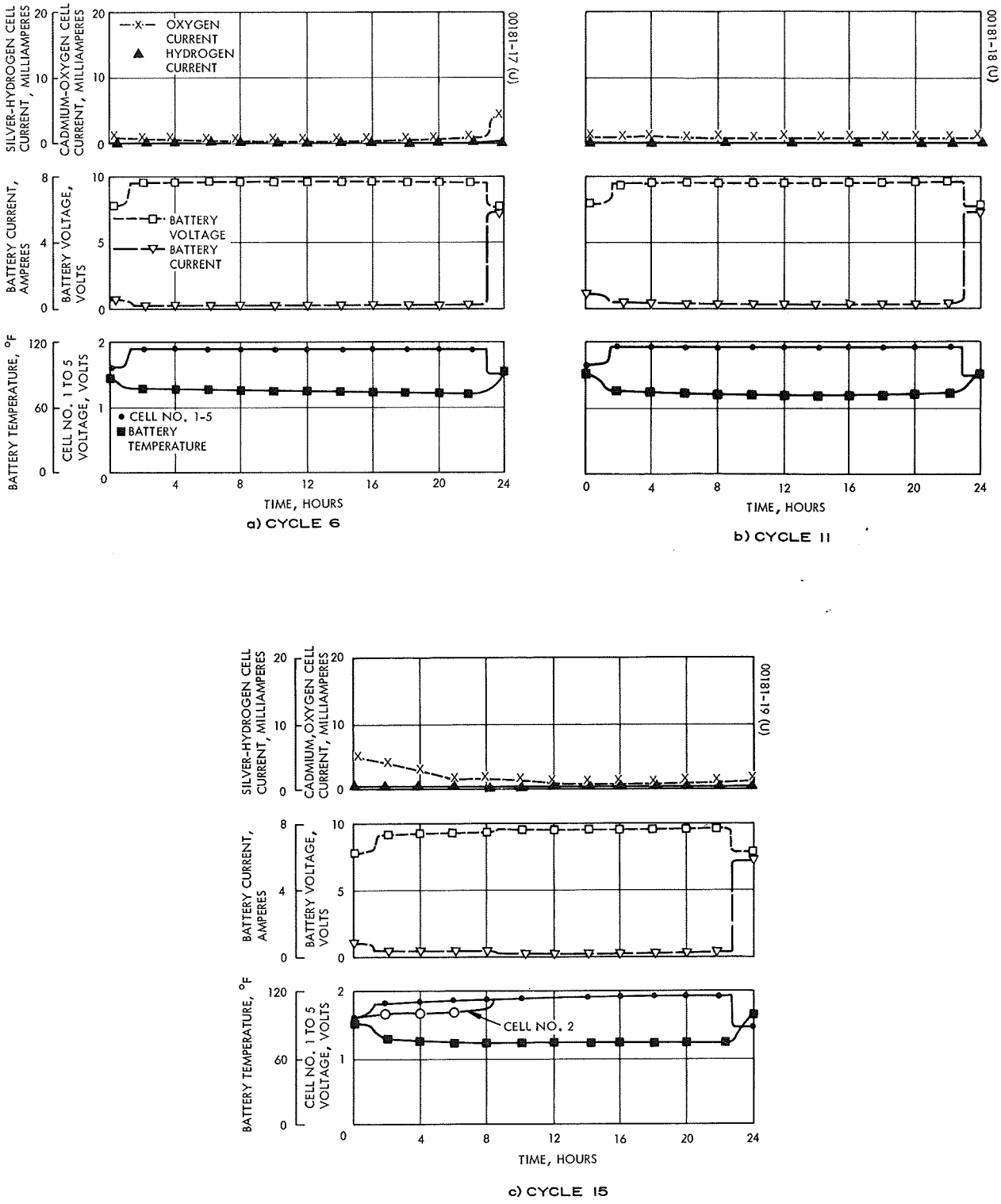

Figure 15. Serial No. 1 Battery Charge - Discharge Cycle at 77°F with Gas Recombination Cells

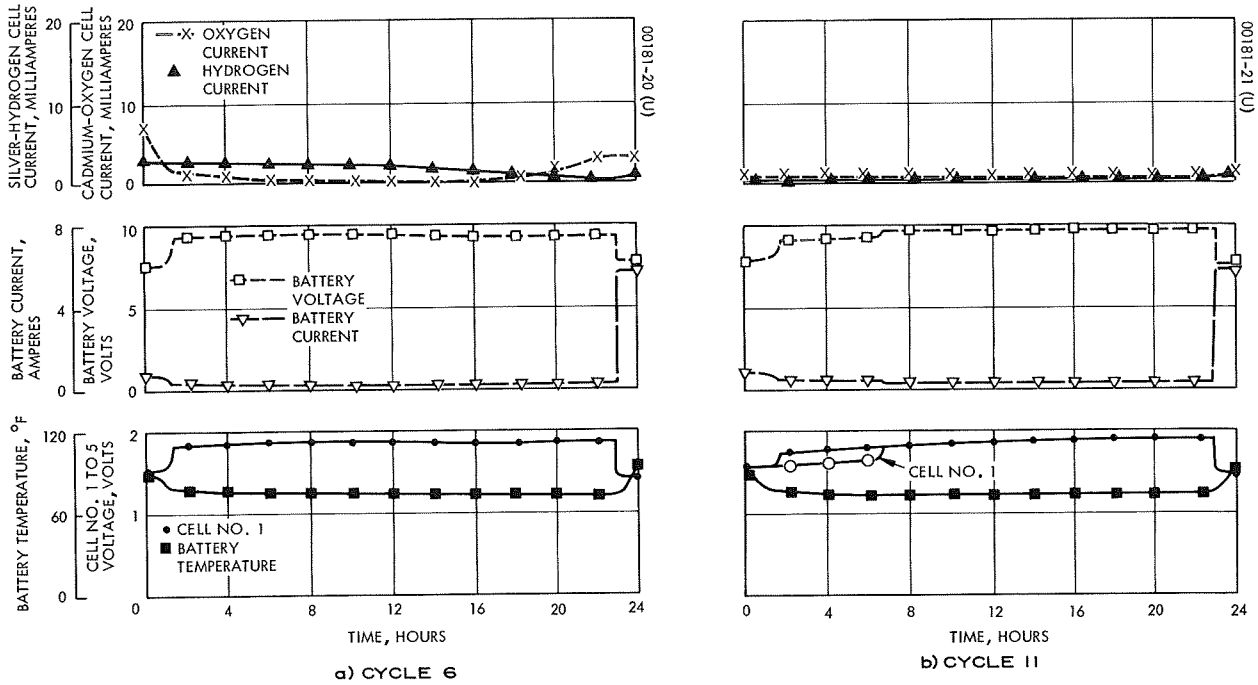

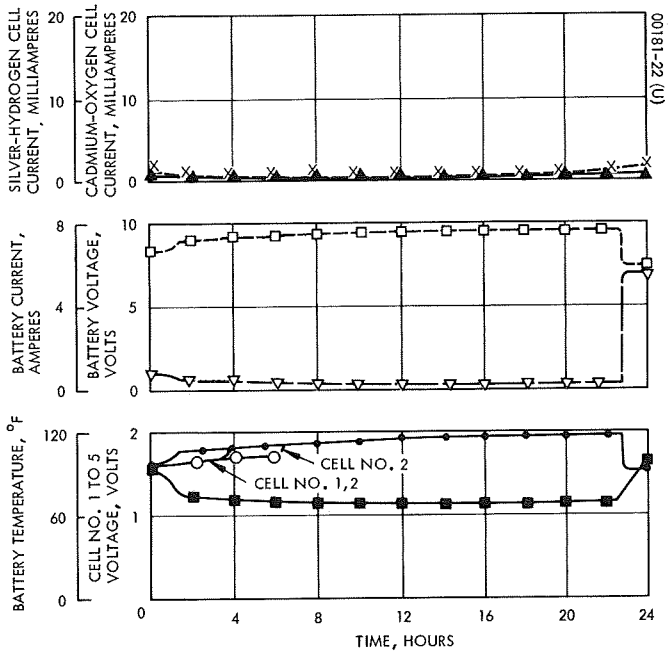

Figure 16. Serial No. 5 Battery Charge - Discharge Cycle at 77°F with Gas Recombination Cells

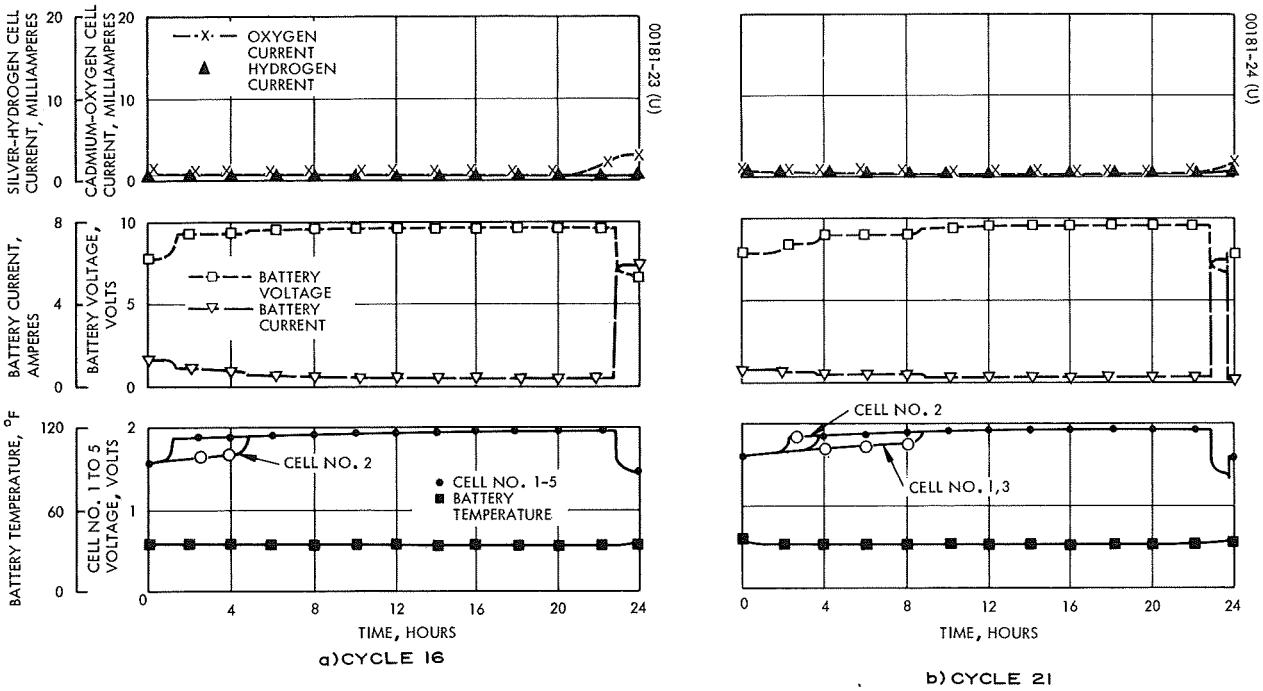

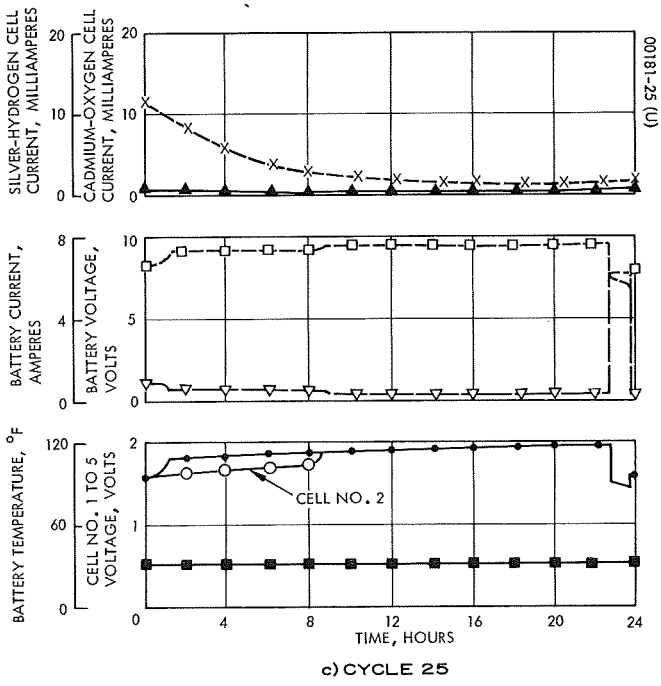

Figure 17. Serial No. 1 Battery Charge - Discharge Cycle at 32°F with Gas Recombination Cells

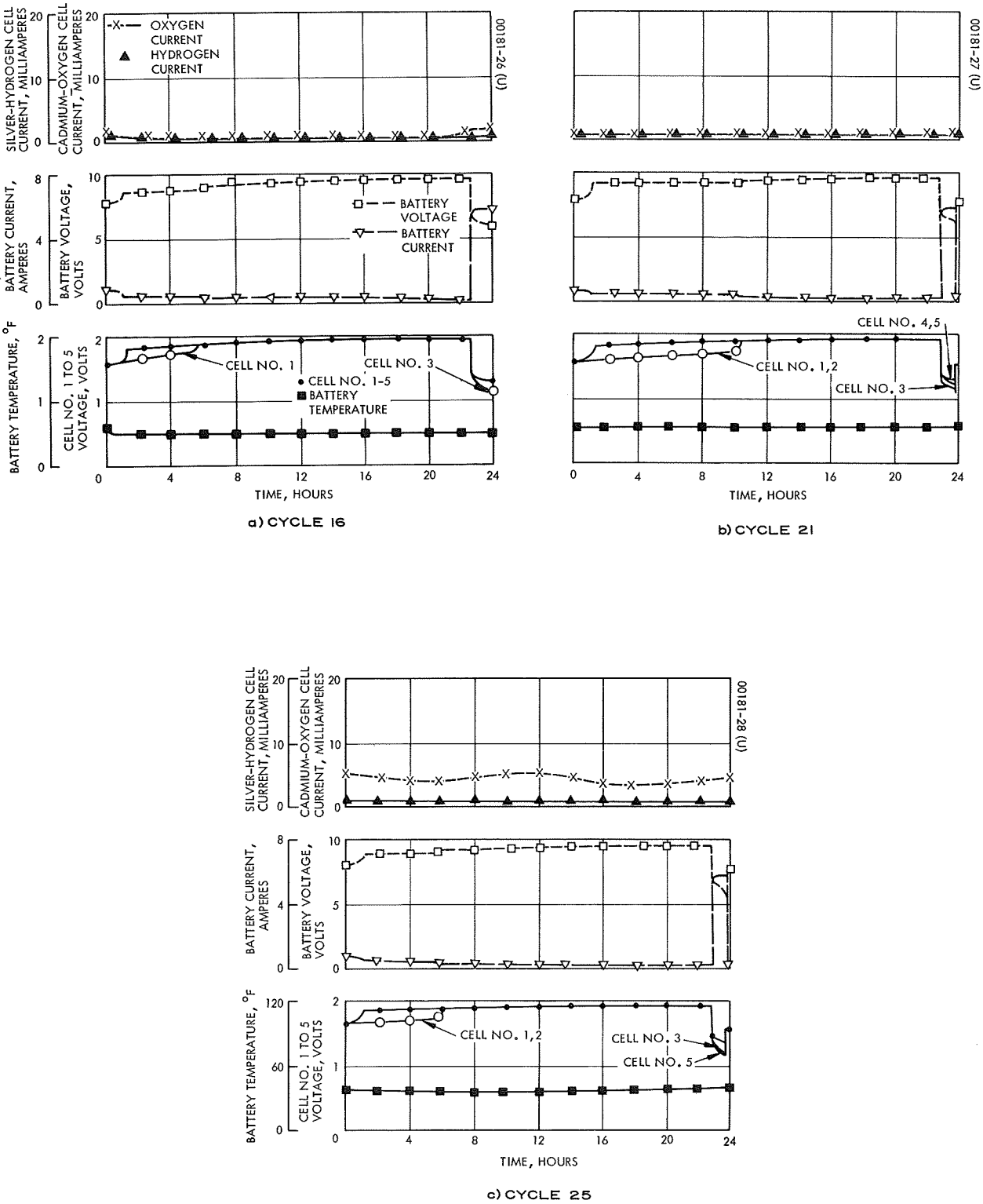

Figure 18. Serial No. 5 Battery Charge - Discharge Cycle at 32°F with Gas Recombination Cells

During and at the conclusion of the tenth 24-hour test cycle at 25° C, both batteries 1 and 5 delivered well in excess of the required 12 amp-hr. However, both batteries failed to deliver the required 7.2 amperes for 1.0 hour under the ambient temperature condition of 0° C. The batteries were cycled through ten charge-discharge cycles at 0° C, but discharge was terminated at a 1.00 volt per cell cutoff. At the conclusion of the last discharge cycle at 0° C, both batteries were charged at 25° C and then were discharged to determine their stored ampere-hour capacity to a 1.00 volt per cell cutoff. Battery No. 1 delivered 17.3 amp-hr and battery No. 5 delivered 7.3 amp-hr. Because the acceptance criterion at this point required 12 amp-hr minimum, this battery was failure analyzed to determine the cause of its poor performance.

2.3 BATTERY FAILURES

In an attempt to include many different improvements into the batteries for this program, each having their own individual merit, some of the detrimental interactions were not accommodated. In particular, it is a drastic step to eliminate the standard "U" folded separator configuration from a silver-zinc cell, but the improved separator-plate-electrolyte interface produced is desirable. It was found that the separator frame core fabrication is reproducible and reliable when inexpensive but necessary tooling is used. However, in an attempt to prevent or to reduce the rate of zinc oxide plate edge crumbling that would result in the loss of active materials to the cell, the negative plates included a 0.25 inch foldback of the 2/0 Exmet silver grid. This foldback or double thickness of expanded metal grid amounted to about 0.035 inch in thickness, and therefore when compressed to the final plate thickness of 0.029 inch, it left expanded metal grid right at the plate surface in this foldback region at the periphery of each negative plate. This, combined with the mechanical clamping operation required during the fabrication of the cell cores and the vulnerability of the Permion 2291 polyethylene separator to punctures, all combined to produce a series of small holes through the separator system.

These punctures of the separator system occurred while the cell cores were clamped for the application of epoxy around the periphery of the separator frames and the subsequent oven curing of this epoxy. This was a suspect area anticipated at the time this fabrication step was performed. Resistance measurements were taken on each cell core after removal from the tooling following the epoxy operation and again after insertion of each cell core into its cavity in the monoblock case. Unfortunately, this should have been done while the cell cores still were in their clamped condition. These measurements might have been significant at that point. The expanded metal in the foldback region pierced the separator system, particularly the Permion 2291, and upon removal of the clamps, these pierce points retracted. The damage was not detected until the batteries were activated and electrically cycled.

2.3.1 Performance Symptoms

Batteries 2, 4, 5 and 6 all exhibited similar symptoms prior to their irreversible failure to deliver acceptable capacity. In some cases, the symptoms just required a greater number of charge-discharge cycles to present themselves. In these batteries, one, two, or three cells during charge would not achieve voltages much above 1.8 volts initially. Subsequent charge-discharge cycling would cause this on-charge voltage maximum to drop still further until it was less than 1.0 volt. Finally, the defective cells would exhibit reversed voltages because the cell completely shorted and therefore the recorded voltage actually was that of the respective cell terminals of adjoining cells in the battery. As soon as one or more cells started to fail in this manner within a battery, that battery could not deliver acceptable capacity on discharge. If a complete short occurred, there was no available capacity; a partial short discharged the battery internally, producing reduced deliverable ampere-hour capacity.

2.3.2 Autopsy Results

Careful microscopic examination of failed cells showed that there was a series of punctures through the Permion 2291 separator system almost entirely in the region where the 0.25 inch foldback of the negative plate expanded metal grid was located. In a few cases, zinc dendrites were observed in the central portion of the separator; these were random cases, probably caused by the separator system being pierced during cell core fabrication.

Another significant observation was the fact that there was severe zinc plate slumping. This was not totally unexpected because during the first formation cycle it became necessary to use metal plates bolted across the batteries to prevent distortion of the end walls of the monoblock case. The foldback of the expanded metal grid and the use of teflon in the negative plates both were used to minimize this problem. As far as could be ascertained, teflonation of the negative plates has little or no affect upon reducing or preventing zinc plate slumping. The outermost cells were the worst, the second and fourth cells were not quite as bad, and the center cell was the best with regard to zinc plate slumping. Further, it is interesting to note, concerning the cells that failed by shorting, cell numbers 2 and 4 appeared to be preferential candidates.

The Permion 2291 separator was measured for swell in the presence of 40 weight percent potassium hydroxide solution. Its swell factor is 5 percent. Previously, Permion 2290 was measured and it swells by a factor of 10 percent under the same conditions. This compares with cellulosic materials that exhibit swell factors in the range of 300 to 500 percent in concentrated potassium hydroxide solutions. The proper mechanical support of the zinc electrodes is essential in minimizing the slumping problem. In worst case situations, it appeared that the upper third to upper half of the silver and zinc plates were not being utilized electrochemically because of the slumping problem.

2.3.3 Seal Integrity

Batteries 1, 2A, and 3 developed electrolyte leakage problems after shipment to Goddard Space Flight Center. This leakage occurred at three locations:

1) The case-to-cover epoxy bond just above the connector (refer to Figure 12)

2) The epoxy encapsulated wiring channels (refer to Figure 10)

3) The epoxy bond between the plastic tube from the gas recombination assembly and the common gas manifold (refer to Figures 10 and 11)

The case-to-cover epoxy bond probably fractured because of internal pressure that developed within the battery. This could have been caused by the mechanical pressure that was present, attributable to the zinc-zinc oxide electrochemical reaction during battery capacity cycling, or by subsequent hydrogen gas generation within the battery caused by zinc reacting with electrolyte during open circuit stand for an extended period. Because the support plates covered only the lower half of the end walls of the battery, any internal pressure that developed within the battery could act upon the case-to-cover epoxy bond.

The leakage that developed at the end of the two wiring bundles apparently followed a capillary path along the silver plate tabs, through the epoxy encapsulation, along the teflon insulated wire, and finally out the end of the wiring channels. This occurred even though the leakage path was tortuous. Specially designed terminal seals will eliminate this problem in the phase III batteries.

The gas recombination assembly was mounted to permit the use of the support plates at each end of the five-cell battery. Because of these support plates, the only adhesive bonding possible between the battery and the gas recombination assembly was at the point of attachment of the acrylic tube to the common gas manifold and at the contiguous surfaces of the microfuel cell and the end wall of the battery. Further, it was considered desirable to be able to readily separate the gas recombination assembly from the battery without damage to either part. Therefore, the bond between the microfuel cell and the end wall of the battery was purposely made to fracture easily. Unfortunately, this permits high stress to develop in the epoxy bond between the acrylic tube and the common gas manifold - which probably caused the electrolyte leakage observed there.

3.0 NEW TECHNOLOGY

The phase of the program reported herein was primarily a fabrication and test period. The only item that may be considered as possible new technology is the use of the microporous hydrophobic membrane to separate gases and electrolyte, as reported in subsection 2.1.4.

4.0 PROGRAM FOR NEXT REPORTING PERIOD

This contract has been extended by Goddard Space Flight Center through December 1970. A change in the scope of work will include the design, fabrication, and testing of six, five-cell batteries incorporating injection molded single cell cases rather than the five-cell monoblock battery cases used to date. These batteries will be 12 amp-hr size and will include the same type of cell core construction developed on this program with two different separator material or configuration selections. Some experimental cells will be designed, fabricated, and tested that will include the same cell core construction but will eliminate the injection molded case by conformally coating the cell core itself and then encapsulating it into epoxy. This construction will produce a "zero" draft angle cell jar. Design details for the next period still are in formulative stages, but Section 5.0 comments on some of the items under consideration for the next period.

5.0 CONCLUSIONS AND RECOMMENDATIONS

5.1 CELL CORE CONSTRUCTION

The cell core construction developed on this program eliminates the "U" fold separator configuration, thereby improving the plate-separator geometry. With inexpensive yet adequate tooling cell core fabrication can be readily accomplished on an R&D, pilot line or high production rate basis. The difficulties encountered with the piercing of the separator were related to the metal grid geometry in the negative plates. Hughes definitely recommends that this cell core construction has potential for improving the performance of high reliability silver-zinc cells required for space, military, or commercial applications.

5.2 TEFLONATED NEGATIVE PLATES

Hughes experience with the teflonated plates used to date would indicate that there is no improvement over non-teflonated plates with respect to producing lower rates of zinc plate slumping. Hughes does not recommend the use of teflonated zinc plates for the next phase of this contract.

5.3 GAS RECOMBINATION ASSEMBLY

This assembly is very difficult to incorporate and then to operate without extensive programming being incorporated into a spacecraft's charge control system. The problem of gas generation during recharge of the microfuel cell, the fact that the charge scheme used for the silver-zinc battery did not produce intolerable amounts of oxygen, incorporation and operational complexity, all lead to the recommendation that the gas recombination assembly not be used for the next period of this contract.

5.4 SEPARATOR SYSTEM

The severe zinc plate slumping probably was brought about because of the low swell factor polyethylene separator. Silver migration was not a problem and there was no indication of zinc dendrites penetrating the Permion 2291 in the batteries that were autopsied except where the separator system was previously punctured. This material must be incorporated into silver-zinc cells in a manner that optimizes its

performance, and not in a manner that necessarily is similar to the way other separator materials, such as cellulosic materials, have been used in the past. The poor low temperature performance of the batteries tested to date can be attributed to the higher resistivity of the Permion 2291. Hughes recommends that the separator configuration be improved during the next phase of this contract by the use of other materials in conjunction with the Permion 2291, such as cellulosic and/or potassium titanate materials for zinc plate support, and that the number of layers of Permion 2291 possibly should be reduced to improve low temperature performance.

5.5 MONOBLOCK CASE

The thin-wall, five-cavity, minimum interior wall draft angle battery case pushed state-of-the-art injection molding practice to its feasibility limits. For the next period, a single cell case is recommended, still with minimum interior draft angle, but with thicker walls.

5.6 COVER

A less complex cover can be used on a single cell jar.

5.7 MICROPOROUS HYDROPHOBIC MEMBRANE

This membrane is excellent for applications where gases and aqueous solutions must be separated. Water loss will not occur if the partial pressure of water vapor is the same on both sides of the membrane; however, this type of membrane could not simply be installed on the top of a silver-zinc cell where the external surface of the membrane is exposed to an air or vacuum environment.

APPENDIX I. STATISTICAL SUMMARY OF SILVER AND ZINC OXIDE PLATE DATA

The data shown represents measurements taken at Hughes Aircraft Company. The electrical connection tabs of each plate were randomly cut to length within ±0.1 inch tolerance. Therefore, the thickness data is accurate, but there is a greater range shown in the weight measurements than is actually the case.

Number	Mean	σ	R_{LO}	R_{HI}
Mass of Zinc Oxide Plates – Grams				
147	10.8721	0.1741	10.42	11.49
Mass of Silver Plates – Grams				
176	10.4235	0.2001	10.01	10.88
Mass of Silver Plates Before $Ca(OH)_2$ Plating – Grams				
72	10.422	0.2031	10.01	10.88
Mass of Silver Plates After $Ca(OH)_2$ Plating – Grams				
72	10.793	0.2496	10.35	11.50

Thickness of Zinc Oxide Plates

N	149	149	149	447	
$\bar{X}$	0.03725	0.03713	0.03697	0.037114	
σ	0.00221	0.00187	0.00225	0.00211	
R_{HI}	0.043	0.042	0.043	0.043	
R_{LO}	0.032	0.033	0.032	0.032	
	Top	Middle	Bottom	Total	

Thickness of Silver Plates

N	145	145	145	435	
$\bar{X}$	0.02156	0.02157	0.02153	0.02155	
σ	0.00044	0.00041	0.00052	0.00046	
R_{HI}	0.0224	0.0225	0.0224	0.0225	
R_{LO}	0.0198	0.0201	0.0196	0.0196	
	Top	Middle	Bottom	Total	

Thickness of Silver Plates With
$Ca(OH)_2$ Plating

N_I	109	109	109	327	
N_F	109	109	109	327	
$\overline{X}_I$	0.02149	0.02145	0.02139	0.02444	1.32 mil
$\overline{X}_F$	0.02279	0.02277	0.02271	0.02276	
σ_I	0.00042	0.00039	0.00053	0.00045	
σ_F	0.00044	0.00039	0.00043	0.00042	
R_{LO_I}	0.0198	0.0201	0.0196	0.0196	
R_{LO_F}	0.0215	0.0215	0.219	0.0219	
R_{HI_I}	0.0222	0.0224	0.0221	0.0224	
R_{HI_F}	0.0240	0.0240	0.0240	0.0240	
	Top	Middle	Bottom	Total	Mean Plating Thickness